

# Organometallic vapor-phase epitaxy of $\text{Hg}_{1-x}\text{Cd}_x\text{Te}$ on {211}-oriented substrates

M. J. Bevan, N. J. Doyle, and T. A. Temofonte

Citation: **71**, 204 (1992); doi: 10.1063/1.350743

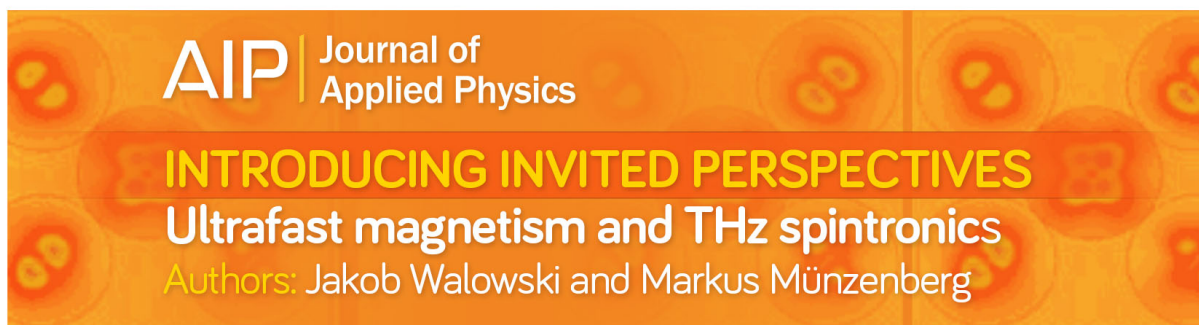
View online: <http://dx.doi.org/10.1063/1.350743>

View Table of Contents: <http://aip.scitation.org/toc/jap/71/1>

Published by the American Institute of Physics

---

---



**AIP** | Journal of  
Applied Physics

**INTRODUCING INVITED PERSPECTIVES**

**Ultrafast magnetism and THz spintronics**

Authors: Jakob Walowski and Markus Münzenberg

# Organometallic vapor-phase epitaxy of $\text{Hg}_{1-x}\text{Cd}_x\text{Te}$ on {211}-oriented substrates

M. J. Bevan, N. J. Doyle, and T. A. Temofonte  
*Westinghouse Science & Technology Center, Pittsburgh, Pennsylvania 15235*

(Received 3 December 1990; accepted for publication 20 September 1991)

$\text{Hg}_{1-x}\text{Cd}_x\text{Te}$  layers have been grown by organometallic vapor-phase epitaxy at 350 °C on {211}-oriented substrates, including CdTe, (CdZn)Te, and GaAs, with the emphasis on lattice matching for improved structural quality films. Characterization included optical microscopy, x-ray diffraction, Fourier transform infrared spectroscopy, and detailed field and temperature Hall measurements. The (211)*B*-oriented epilayers combine the structural quality of (100) including the absence of twinning with the flat topography of (111)*B*-oriented films. The crystal quality improved to that of the substrate with the closer lattice matching of (CdZn)Te, the mismatch taken up with lattice inclination on the high step density surface. A tighter control of the substrates' Zn content than exists at present is required for ultimate lattice matching to  $\text{Hg}_{0.2}\text{Cd}_{0.8}\text{Te}$ . As-grown  $\text{Hg}_{1-x}\text{Cd}_x\text{Te}$  on (CdZn)Te (211)*B* substrates is *p* type with carrier levels in the  $1\text{--}6 \times 10^{16}\text{cm}^{-3}$  range for compositions greater than 0.20 and with no indication of mixed conduction behavior due to inversion layers or growth-related surface or interface layers.

## I. INTRODUCTION

Epitaxy of III-V compounds is best performed in the (100) orientation, although there are some peculiar physical properties of heterostructures grown along the [111] direction under study.<sup>1,2</sup> For II-VI compounds, especially for the ternary alloy  $\text{Hg}_{1-x}\text{Cd}_x\text{Te}$ , the (111)*B* orientation remains attractive as the growth results in flat, featureless surfaces and heterostructures with excellent interfaces with lattice-matched (e.g., (CdZn)Te) or highly mismatched (e.g., GaAs) substrates.<sup>3–13</sup> In contrast, mercury cadmium telluride of the (100) orientation grown by organometallic vapor-phase epitaxy (OMVPE) is free of microtwins, but exhibits a high density of hillocks (typically,  $10^2\text{--}10^5\text{cm}^{-2}$ )<sup>14,15</sup> and large variations of composition may be associated with these morphological disturbances.<sup>12</sup> The (111)-oriented films have a lamellar twinned structure, giving rise to inferior crystal quality compared to (100) and also degrade its electrical performance. Both photoconductive and photovoltaic devices have been fabricated in (111) layers and have shown reasonable performance as have devices made in (100) epilayers,<sup>12</sup> despite the difference in nature of their defects. However, the ultimate quality and uniformity of (HgCd)Te detector arrays are thought to be limited by structural defects in the films, some of which are generated from structural imperfections in the substrate or from lattice-mismatch stress. Recently, several groups have investigated the growth of (HgCd)Te in other crystallographic directions,<sup>16–20</sup> and this paper explores the use of the {211}-oriented substrates for OMVPE growth of this II-VI semiconductor.

## II. EXPERIMENTAL APPROACH

The OMVPE growth technique used in this work is based on the interdiffused multilayer process (IMP). Details of this and the experimental arrangement have been previously described in detail.<sup>8,9,14</sup> The growth conditions were as follows: substrate temperature of 350 °C, hydrogen

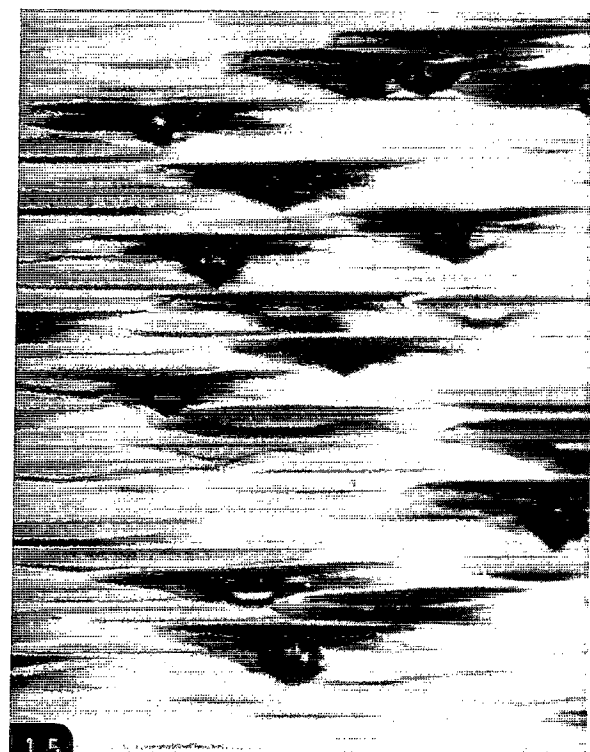
flows of 1.0 and 4.0 slpm during HgTe and CdTe growth, respectively, and partial pressures of DIPTe, DMCd, and elemental Hg of  $1\text{--}3 \times 10^{-3}$ ,  $1 \times 10^{-3}$ , and 0.05–0.1 atm, respectively. Typical growth rates of between 10 and 15  $\mu\text{m/h}$  were used. The (CdZn)Te (nominal Zn 4.5%) and CdTe wafers were oriented {211}, and were chemically polished and free etched in 1% bromine in methanol prior to growth. Some GaAs (211)*B* wafers were used for comparison, although the emphasis was on the use of lattice-matched substrates.

Characterization of the epilayers involved Fourier transform infrared (FTIR) spectroscopy to determine both its thickness and composition. Oscillation photographs were taken with a Nonius Weissenberg x-ray camera with the symmetry direction [111] parallel to the rotation axis and oscillated between 6° and 60° from the sample surface.<sup>21</sup> The film's crystal quality was further examined using a double-crystal diffractometer (Blake Industries). Full width at half-maximum (FWHM) values for the (422) Bragg diffraction ( $\text{CuK}\alpha_1$  radiation) were measured against a Si (100) reference crystal, probing an area of 2  $\text{mm}^2$ .

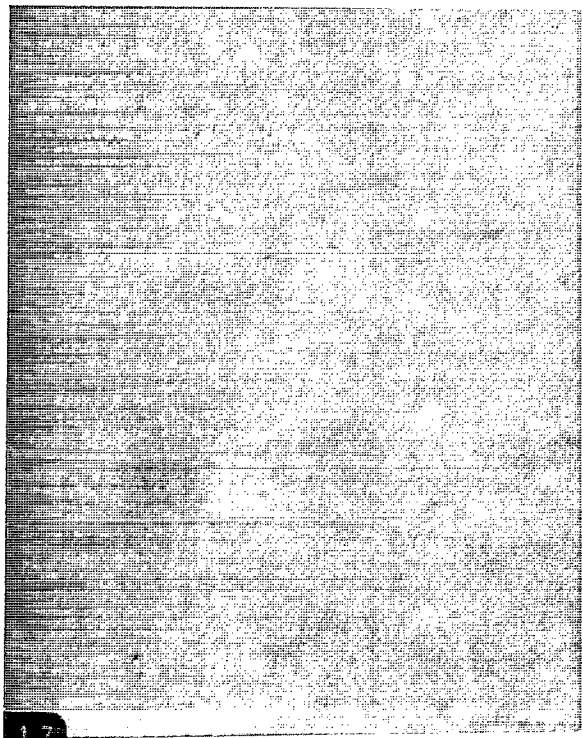
The electrical properties of the (HgCd)Te films were determined by Hall measurements with the van der Pauw method and magnetic-field strengths of 1.2, 2.5, and 5 kG. Measurements were made at 300 and 77 K on  $5 \times 5\text{-mm}^2$  samples with indium contacts. Selected samples were further characterized with a highly automated, multispecimen Hall measurement system, that performs both variable temperature (down to 10 K) and variable field (up to 50 kG using a superconducting magnet) scans.

## III. RESULTS AND DISCUSSION

For (HgCd)Te growth on {111}-oriented substrates, there is a marked difference in surface morphology between the *A* (Cd rich) and *B* (Te rich) faces, the former covered with triangular and hexagonal hillocks, and the



(a) — 10 μm



(b) — 10 μm

FIG. 1. Morphology of  $\text{Hg}_{1-x}\text{Cd}_x\text{Te}$  samples grown on (a)  $(\text{CdZn})\text{Te}$   $(211)A$  and (b)  $(\text{CdZn})\text{Te}$   $(211)B$  substrates. Magnification is  $400\times$ .

latter devoid of features and specular.<sup>22</sup> The same marked contrast applies to the  $\{211\}$  orientation, and Fig. 1 shows the surface morphology of the  $A$  and  $B$  faces, grown in the same run. The  $(211)A$  films exhibit a very rough, terraced

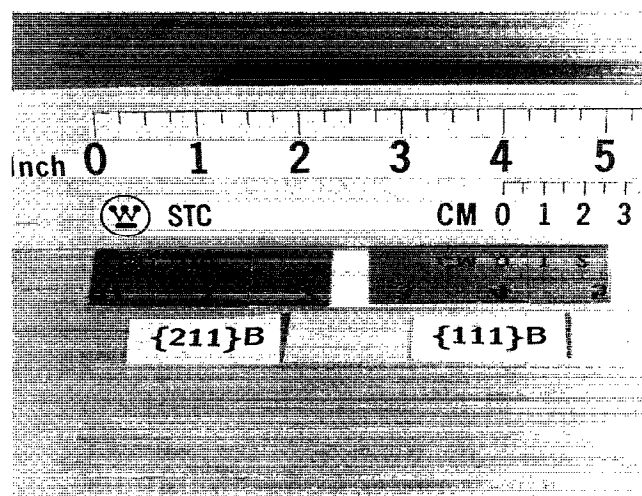
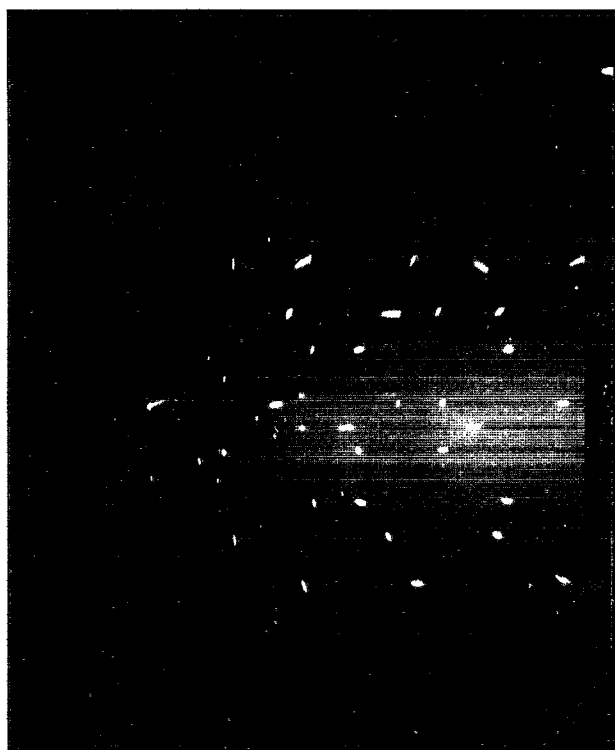


FIG. 2. Photograph showing similarities between  $\text{Hg}_{1-x}\text{Cd}_x\text{Te}$  epilayers deposited on  $(\text{CdZn})\text{Te}$   $(111)B$ - and  $(211)B$ -oriented substrates.

surface compared with the smoother morphology of the  $(211)B$  orientation. The latter has a fine microtexture when compared with that of  $(111)B$  films; but, at lower magnification, there appears little difference as shown in Fig. 2. Similar observations for OMVPE growth have been reported by Cinader and co-workers, who also observed a reduction of deposition rate on the  $A$  face.<sup>18</sup> Twinning occurred in  $(\text{HgCd})\text{Te}$  grown on  $(211)A$  substrates, but was always absent from  $(211)B$  epilayers, in marked contrast to the  $(111)B$  orientation. Figure 3 shows oscillation photographs from two  $(\text{HgCd})\text{Te}$  films grown simultaneously on the two polar faces of  $(\text{CdZn})\text{Te}$   $\{211\}$  substrates. The additional weak reflections between the row lines in Fig. 3(a) are caused by twins in the  $(211)A$  film.

Further investigation of the epilayers with double-crystal diffractometry revealed incomplete parallel growth and variable interplanar tilts. Thin  $(\text{HgCd})\text{Te}$  films ( $3\text{--}4\text{ }\mu\text{m}$ ) were grown for the x-ray beam to penetrate to the substrate and provide information on the incoherent nature of the epilayers. Figure 4(a) shows a  $\text{CuK}\alpha$  (422) rocking curve of an OMVPE layer of  $\text{Hg}_{1-x}\text{Cd}_x\text{Te}$  ( $x = 0.299$ ) on a  $(\text{CdZn})\text{Te}$   $(211)B$  substrate showing both film and substrate peaks. The sample was mounted with the nearest  $[111]$  toward the monochromator. Figure 4(b) shows the effect of reversing the x-ray beam direction, achieved by rotating the sample through  $180^\circ$ .<sup>21</sup> The  $(\text{HgCd})\text{Te}$  epilayer is tilted approximately  $15\text{ arcsec}$  toward the nearest  $(111)$  plane and is not precisely lattice matched to the substrate. Although the zinc content was nominally  $4.5\%$ , the actual value may be between  $3.5\%$  and  $5.5\%$  for wafers from the same  $(\text{CdZn})\text{Te}$  boule and will be lattice matched to  $\text{Hg}_{1-x}\text{Cd}_x\text{Te}$  ( $x = 0.35$ ) or  $\text{HgTe}$ , respectively.<sup>15</sup> The Zn content of individual substrates was not assessed. From the average peak separation  $\Delta\Theta$  of  $133\text{ arcsec}$ , the zinc content appears to be close to  $5.5\%$ , assuming an unstrained  $(\text{HgCd})\text{Te}$  film. The following notation for the separation of the Bragg angle  $\Theta$  is used:

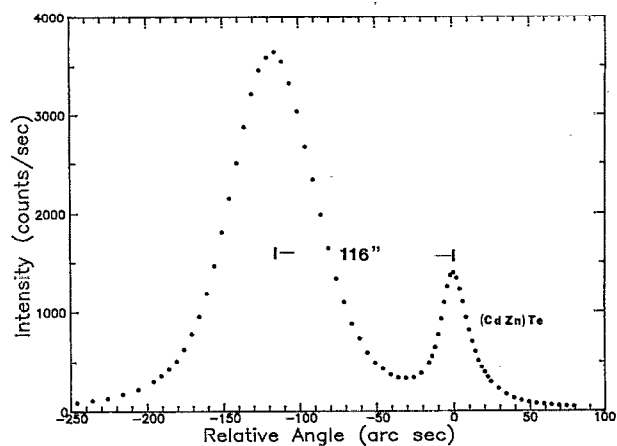


(a)

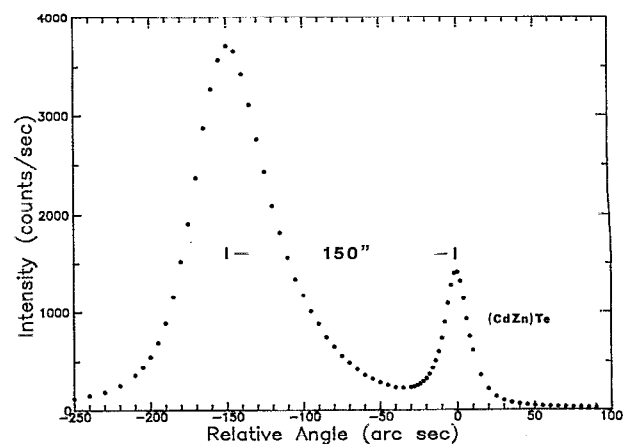


(b)

FIG. 3. Typical oscillation patterns from OMVPE  $\text{Hg}_{1-x}\text{Cd}_x\text{Te}$  on (a)  $(\text{CdZn})\text{Te}$  (211)*A* and (b)  $(\text{CdZn})\text{Te}$  (211)*B* substrates ( $\text{CuK}\alpha_1$  radiation,  $[111]$  rotation axis). The additional weak reflections in (a) are a result of twins.



(a)



(b)

FIG. 4. Double-crystal rocking curve of  $\text{Hg}_{1-x}\text{Cd}_x\text{Te}$  film ( $x = 0.299$ ) on a  $(\text{CdZn})\text{Te}$  (211)*B* substrate using (422) reflection and  $\text{CuK}\alpha_1$  radiation and measured for two azimuths ( $180^\circ$  apart). In (a), nearest  $[111]$  is toward the monochromator and in (b), it is rotated away by  $180^\circ$ .

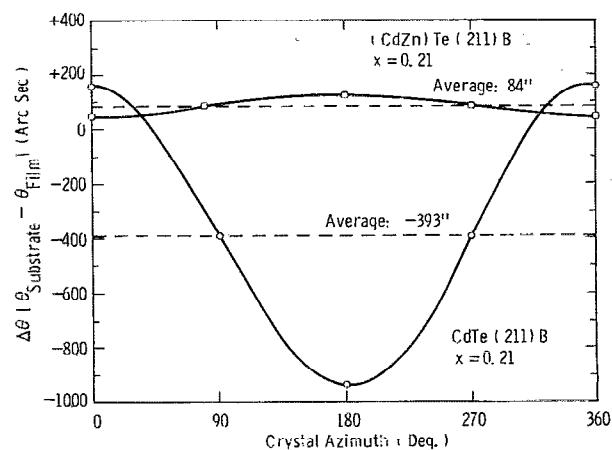


FIG. 5. Peak separations as a function of azimuth for OMVPE  $\text{Hg}_{1-x}\text{Cd}_x\text{Te}$  on  $(\text{CdZn})\text{Te}$  (211)*B* and  $\text{CdTe}$  (211)*B* with  $\text{CuK}\alpha$  (422) reflection and nearest  $[111]$  toward the monochromator.



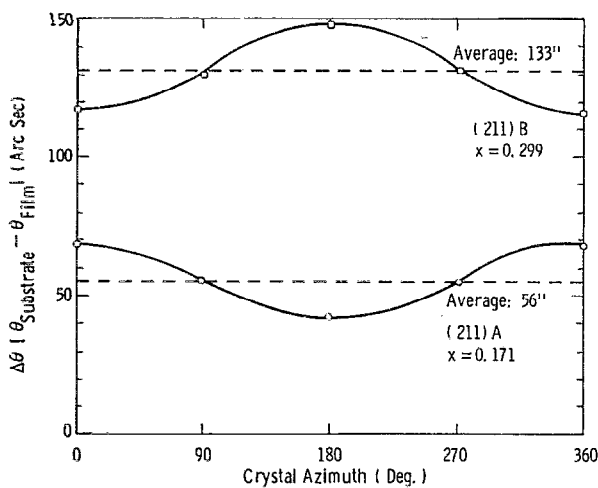


FIG. 6. Peak separations as a function of azimuth for OMVPE  $\text{Hg}_{1-x}\text{Cd}_x\text{Te}$  on (CdZn)Te (211)*A* and (CdZn)Te (211)*B* with  $\text{CuK}\alpha$  (422) reflection and nearest [111] towards the monochromator.

$$\Delta\theta = \theta(\text{substrate}) - \theta(\text{film}).$$

Figure 5 shows the variation of the peak separations at different crystal azimuths for  $\text{Hg}_{1-x}\text{Cd}_x\text{Te}$  films ( $x = 0.202$ ) on both (CdZn)Te (211)*B* and CdTe (211)*B* substrates. The lattice mismatch is greater for the CdTe substrate (0.3%), resulting in both a larger  $\Delta\theta$  ( $-393$  arcsec) and tilt ( $\sim 550$  arcsec toward nearest (111)). The addition of Zn or Hg to CdTe has the effect of reducing the lattice parameter and increasing the Bragg angle.

For the two samples depicted in Fig. 3 and grown on (CdZn)Te (211) *A* and *B* substrates, their compositions were 0.17 and 0.30 respectively, the difference resulting from the slower CdTe growth rate on the *A* face. Figure 6 shows the variation of peak separation with crystal azimuth for both of these films. Both samples show similar tilts (15–20 arcsec) and the difference in compositions is reflected in the average  $\Delta\theta$  values, both consistent with a zinc content of about 5% in the substrate. To confirm that the lattice inclination was connected with the extent of lattice matching with the substrate, (HgCd)Te was deposited on GaAs (211)*B* using a 3–4  $\mu\text{m}$  CdTe buffer grown

sequentially in the same run. The crystal quality (FWHM  $\sim 195$  arcsec) was inferior to that using (CdZn)Te and the extent of the tilt increased to approximately  $4.5^\circ$ . The data are summarized in Table I. The rocking curve widths of the epilayers were typically in the range 40–70 arcsec on the (CdZn)Te (211)*B* substrates, increasing for the larger mismatched substrates, CdTe and GaAs. As the Bragg angle differences  $\Delta\theta$  indicated that the Zn content in the (CdZn)Te substrates was such that they would be lattice matched to HgTe, a HgTe layer was grown on a substrate in which the (HgCd)Te layer had been removed. Coherent growth was confirmed by double-crystal diffractometry, a single, symmetric peak being observed with the lowest FWHM value of 29 arcsec on a substrate that had a FWHM value of 20 arcsec.

In heteroepitaxial systems, the mismatch between the lattice constants can be accommodated by bending of the structure, deformation of the crystal lattice, generation of misfit dislocations at the interface or by inclination of the epitaxial crystal. Inclination of the epitaxial orientation has been observed to relieve the lattice mismatch for III-V growth on (100)-oriented substrates in addition to tetragonal distortion.<sup>23</sup> Substrate misorientation has been found to improve both the morphological as well as the crystal quality in systems including ZnSe on GaAs,<sup>24</sup> CdTe on GaAs,<sup>25</sup> and (HgCd)Te on CdTe.<sup>26</sup> When the substrate is misoriented, the periodic arrangement of steps provides nucleation sites and the mismatch is accommodated in plane by lattice deformation and perpendicular by layer rotation.<sup>23</sup> In this study, this was the case for {211} which is oriented  $19^\circ 28'$  from the nearest {111}. Figure 7 shows the atomic configuration at an idealized abrupt (211) *A* or *B* surface. Although macroscopically the {211} surface contains equal number of cations (Cd or Zn) and anions (Te), microscopically it can be considered as a combination of low-index facets (100) and (111). Inspection of Fig. 7 shows that the *B* surface has Te atoms with two dangling bonds forming a step and Cd or Zn atoms with one dangling bond forming the other sites. The reverse is observed on the *A* face. The inequivalence of the sites suggests that there would be a marked difference in nucleation behavior between the *A* and *B* surfaces and this has been shown to be the case.

TABLE I. Summary of double-crystal-diffractometry data for OMVPE  $\text{Hg}_{1-x}\text{Cd}_x\text{Te}$  films on {211} substrates, (422) reflection,  $\text{CuK}\alpha_1$  radiation, Si(100) reference crystal, 2-mm<sup>2</sup> area.

Substrate	Composition	Thickness ( $\mu\text{m}$ )	FWHM (arcsec)		$\Delta\theta$ (arcsec)	Tilt (arcsec)	Twins
			Film	Substrate			
CZT (211) <i>B</i>	0.299	3.0	59	20	133	15	No
CZT (211) <i>A</i>	0.171	3.0	140	18	56	13	Yes
CZT (211) <i>B</i>	0.202	2.9	54	19	92	26	No
CZT (211) <i>B</i>	0.208	3.4	44	20	84	40	No
CT (211) <i>B</i>	0.210	3.4	118	34	-393	550	No
GaAs (211) <i>B</i>	0.280	9.0	195	...	...	$4.5^\circ$	No
CZT (211) <i>B</i>	0.0	4.0	29	...	0	0	No

TABLE II. 77-K Hall data for  $\text{Hg}_{1-x}\text{Cd}_x\text{Te}$  OMVPE films on  $(\text{CdZn})\text{Te}$  (211) $B$  substrates.

Composition ( $x$ )	Thickness ( $\mu\text{m}$ )	$B = 5 \text{ kG}$		$B = 2.5 \text{ kG}$		$B = 1.25 \text{ kG}$	
		$p \text{ (cm}^{-3}\text{)}$	$\mu \text{ (cm}^2 \text{V}^{-1} \text{s}^{-1}\text{)}$	$p \text{ (cm}^{-3}\text{)}$	$\mu \text{ (cm}^2 \text{V}^{-1} \text{s}^{-1}\text{)}$	$p \text{ (cm}^{-3}\text{)}$	$\mu \text{ (cm}^2 \text{V}^{-1} \text{s}^{-1}\text{)}$
0.206	3.0	$3.0 \times 10^{16}$	401	$3.2 \times 10^{16}$	383	$3.7 \times 10^{16}$	330
0.210	4.3	$1.5 \times 10^{16}$	595	$1.5 \times 10^{16}$	614	$1.6 \times 10^{16}$	568
0.229	3.0	$3.8 \times 10^{16}$	461	$3.6 \times 10^{16}$	491	$3.5 \times 10^{16}$	509
0.229	3.0	$1.9 \times 10^{16}$	494	$1.8 \times 10^{16}$	511	$1.9 \times 10^{16}$	500
0.231	12.4	$1.6 \times 10^{16}$	533	$1.6 \times 10^{16}$	544	$1.6 \times 10^{16}$	554
0.250	4.0	$1.9 \times 10^{16}$	302	$1.8 \times 10^{16}$	306	$1.8 \times 10^{16}$	311
0.307	9.3	$5.7 \times 10^{16}$	264	$5.8 \times 10^{16}$	258	$6.3 \times 10^{16}$	238

Growth nucleates at the high density of steps on the (211) $B$  surface, Te atoms preferentially bonding to the Cd/Zn atoms at the steps, and prevents the formation of Te clusters, which are thought to be a source of dislocations, stacking faults, and subsequent hillocks.<sup>27</sup> (HgCd)Te in a single twin domain propagates across the surface to the adjacent nucleation site or step. This is in marked contrast to the  $A$  face, as the Te atoms at the steps are not so reactive and there is a tendency to form Te clusters, resulting in twin domains and hillocks. The use of misoriented (100) (CdZn)Te substrates also gives rise to twin-free (HgCd)Te and the degree and direction of the misorientation also controls the density of hillocks.<sup>27</sup> Cadmium steps/terrace edges also appear to be important in the nucleation process on the (100) surface to prevent the formation of hillocks. For growth on (111) $B$  substrates, (HgCd)Te nucleates as islands with individual islands having roughly equal probability of being in either of the two twin-related orientations. Misorientation would provide nucleation steps/terraces, and twin-free (HgCd)Te has been reported for OMVPE growth on  $18^\circ$  off (arbitrary direction) (111) $B$  CdTe substrates.<sup>12</sup> The {211} planes are coincidentally  $19^\circ$  from the nearest {111}.

For growth on (CdZn)Te (211) $B$ , the small amount of observed mismatch (about 0.06%) derived from  $\Delta\Theta$  values is consistent with the amount of inclination of the

(HgCd)Te lattice (20–40 arcsec), as the difference in the lattice constant is taken up across the steps in the surface. Tetragonal deformation is likely to occur with a contraction of the lattice within the plane and an increase in the lattice parameter perpendicular to the surface, but was not verified by using asymmetric reflections. For growth on CdTe (211) $B$  substrates with a larger lattice spacing, the deformation is in the opposite sense, and the inclination ( $550 \text{ arcsec}$ ) is consistent with the need to accommodate the larger mismatch (0.3%). In the case of GaAs, part of the 14.6% mismatch is relieved with a  $4.5^\circ$  tilt of the lattice. Crystal quality of the films as reflected in narrower rocking curve widths improved as the lattice mismatch was reduced. The smallest FWHM values were obtained with HgTe epilayers on (CdZn)Te substrates, which had a higher Zn content than expected. Ghandhi *et al.* reported similar FWHM values for HgTe grown on (CdZn)Te oriented  $2^\circ$  off (100), the Zn content of which gave rise to a  $\Delta\Theta$  value of over  $150 \text{ arcsec}$ .<sup>28</sup> Whereas HgTe on (CdZn)Te (100) $2^\circ$  showed no inclination of the lattice, a tilt of only  $78 \text{ arcsec}$  was observed for growth on CdTe,<sup>29</sup> the small inclination resulting from the longer step lengths compared to {211}.

The electrical behavior of the OMVPE layers was assessed by Hall measurements. As-grown material is  $p$  type at 77 K ( $x > 0.20$ ), dominated by metal vacancies at the growth temperature and the Hg partial pressures used in this study. Table II shows the low-field-dependent Hall data at 77 K for  $\text{Hg}_{1-x}\text{Cd}_x\text{Te}$  films grown with a range of compositions and thicknesses on (CdZn)Te (211) $B$  substrates. The material was  $p$  type with acceptor levels in the range  $1\text{--}6 \times 10^{16} \text{ cm}^{-3}$ , and the lack of significant field dependence indicates no appreciable mixed conduction and therefore no  $n$ -type surface or interface layers in the samples. No intentional dopant was added to the films. Typical detailed temperature and field measurements are shown in Fig. 8 for a thin and low- $x$  (HgCd)Te film, particularly vulnerable to mixed conduction arising from  $n$ -type skins, which can dominate the Hall coefficient due to the unusually high electron/hole mobility ratio in this system. The (HgCd)Te films were terminated with a thin CdTe layer ( $> 0.2 \mu\text{m}$ ), that proved to be a suitable encapsulant to freeze in the Hg vacancies and prevent the formation of any  $n$ -type skins. Classic behavior is observed for the resistivity, carrier concentration, and mobility variations

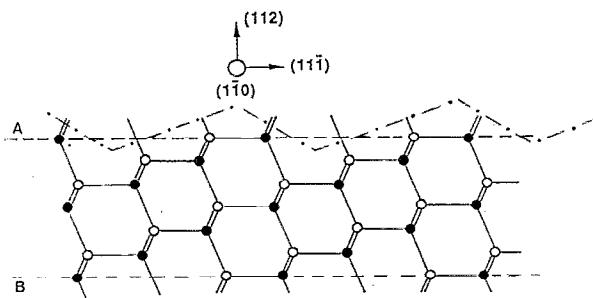


FIG. 7. Atomic arrangements near idealized (CdZn)Te (211)  $A$  and  $B$  surfaces. There are two differently occupied sublattices indicated by black (anion) and white (cation) atoms. The double lines represent two separate bonds connecting each atom shown with two separate atoms in different planes. The dotted zigzag line shows that the surface may be viewed as an alteration of (100) and (111) facets.

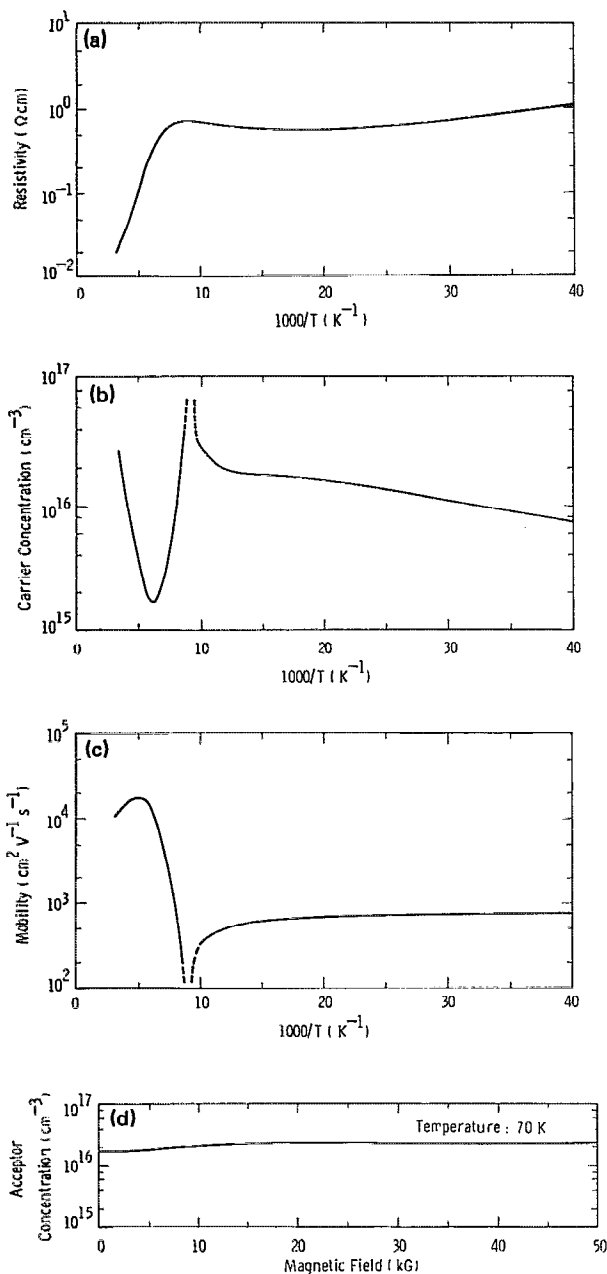


FIG. 8. Classic Hall behavior for low-level ( $p = 2 \times 10^{16} \text{ cm}^{-3}$ ), unintentionally doped  $\text{Hg}_{1-x}\text{Cd}_x\text{Te}$  film ( $x = 0.202$ ,  $t = 4 \mu\text{m}$ ), showing the temperature dependence of (a) resistivity, (b) carrier concentration, and (c) mobility. The observed variation of acceptor concentration with magnetic field at 70 K is shown in (d).

with temperature, as illustrated in Fig. 8. High-field measurements up to 50 kG revealed no evidence of mixed conduction similar to that reported earlier for intentionally doped  $\text{Hg}_{1-x}\text{Cd}_x\text{Te}$  with  $x < 0.20$ .<sup>30</sup> Figure 8(d), for example, shows the lack of any magnetic-field dependence (up to 50 kG) of the acceptor concentration for this film ( $x = 0.202$ ,  $t = 4.0 \mu\text{m}$ ).

#### IV. CONCLUSIONS

OMVPE growth of (HgCd)Te on (211)*B*-oriented substrates avoids the problems of hillock formation ob-

served for (100) growth and twinning seen in (111) films. By using lattice-matched substrate (CdZn)Te, epitaxial films comparable in crystal quality to that of the substrate can be grown at 350 °C. However, the lack of precise control of the zinc content in (CdZn)Te has meant that exact lattice matching cannot be maintained from wafer to wafer. An alternative substrate material is Cd(TeSe), but its purity is such that mobile impurities dope the (HgCd)Te films at the growth temperature utilized.<sup>15</sup> The lattice mismatch is taken up by lattice tilting and possible distortion on this high step density surface. Electrically, the (211)*B*-oriented (HgCd)Te films are *p* type as grown, similar in behavior to (100)-oriented films, and, because of the absence of twinning, there is no evidence of *n*-type behavior as observed for (111)-oriented layers.<sup>12</sup>

#### ACKNOWLEDGMENTS

The authors are much indebted to E. Elkan for substrate polishing and preparation, and C. F. Seiler for assistance with the FTIR and Hall measurement characterization.

- <sup>1</sup>K. Kato, Y. Hasumi, A. Kozen, and J. Temonyo, *J. Appl. Phys.* **65**, 1947 (1989).
- <sup>2</sup>S. Fuke, M. Umemura, N. Yamada, K. Kuwahara, and T. Imai, *J. Appl. Phys.* **68**, 97 (1990).
- <sup>3</sup>S. J. C. Irvine and J. B. Mullin, *J. Cryst. Growth* **55**, 107 (1981).
- <sup>4</sup>W. E. Hoke and R. Traczewski, *J. Appl. Phys.* **54**, 5087 (1983).
- <sup>5</sup>S. K. Ghandhi and I. Bhat, *Appl. Phys. Lett.* **44**, 779 (1984).
- <sup>6</sup>J. L. Schmit, *J. Vac. Sci. Technol. A* **3**, 89 (1985).
- <sup>7</sup>D. D. Edwall, E. R. Gertner, and L. O. Bubulac, *J. Cryst. Growth* **86**, 240 (1988).
- <sup>8</sup>J. Tunncliffe, S. J. C. Irvine, O. D. Dosser, and J. B. Mullin, *J. Cryst. Growth* **68**, 245 (1984).
- <sup>9</sup>M. J. Bevan and K. T. Woodhouse, *J. Cryst. Growth* **68**, 254 (1984).
- <sup>10</sup>P. A. C. Whiffin, B. C. Easton, P. Capper, and C. D. Maxey, *J. Cryst. Growth* **79**, 935 (1986).
- <sup>11</sup>M. J. Hyliands, J. Thompson, M. J. Bevan, K. T. Woodhouse, and V. Vincent, *J. Vac. Sci. Technol. A* **4**, 2217 (1986).
- <sup>12</sup>P. Capper, C. D. Maxey, P. A. C. Whiffin, and B. C. Easton, *J. Cryst. Growth* **96**, 519 (1990).
- <sup>13</sup>S. J. C. Irvine, J. S. Gough, J. Giess, M. J. Gibbs, A. Royle, C. A. Taylor, G. T. Brown, A. M. Keir, and J. B. Mullin, *J. Vac. Sci. Technol. A* **7**, 285 (1989).
- <sup>14</sup>M. J. Bevan, N. J. Doyle, and J. Gregg, *J. Mater. Res.* **5**, 1475 (1990).
- <sup>15</sup>M. J. Bevan, N. J. Doyle, and D. Synder, *J. Cryst. Growth* **102**, 785 (1990).
- <sup>16</sup>L. M. Smith, C. F. Byrne, D. Patel, P. Knowles, J. Thompson, G. T. Jenkin, T. Nguyen Duy, A. Durand, and M. Bourdillot, *J. Vac. Sci. Technol. A* **8**, 1078 (1990).
- <sup>17</sup>W. L. Ahlgren, S. M. Johnson, E. J. Smith, R. P. Ruth, B. C. Johnston, M. H. Kalisher, C. A. Cockrum, T. W. James, D. L. Arney, C. K. Ziegler, and W. Lick, *J. Vac. Sci. Technol. A* **7**, 331 (1989).
- <sup>18</sup>G. Cinader, A. Raizman, and A. Sher, *J. Vac. Sci. Technol. B* **9**, 1634 (1991).
- <sup>19</sup>T. H. Myers, R. W. Yanka, K. A. Harris, A. R. Reisinger, J. Han, S. Hwang, Z. Yang, N. C. Giles, J. W. Cook, J. F. Schetzina, R. W. Green, and S. McDevitt, *J. Vac. Sci. Technol. A* **7**, 300 (1989).
- <sup>20</sup>R. J. Koestner, H.-Y. Liu, H. F. Schaake, and T. R. Hanlon, *J. Vac. Sci. Technol. A* **7**, 517 (1989).
- <sup>21</sup>W. J. Takei and N. J. Doyle, *Mater. Res. Soc. Symp. Proc.* **90**, 189 (1987).
- <sup>22</sup>R. Korenstein, P. Hallock, B. MacLeod, W. Hoke, and S. Oguz, *J. Vac. Sci. Technol. A* **8**, 1039 (1990).
- <sup>23</sup>H. Nagai, *J. Appl. Phys.* **45**, 3789 (1974).
- <sup>24</sup>A. Ohki, N. Shibata, and S. Zembutsu, *J. Appl. Phys.* **64**, 694 (1988).
- <sup>25</sup>E. Ligeon, C. Chami, R. Danielou, G. Feuillet, J. Fontenille, K. Sam-

- inadayar, A. Ponchet, J. Cibert, Y. Gobil, and S. Tatarenko, *J. Appl. Phys.* **67**, 2428 (1990).
- <sup>26</sup>S. M. Johnson, W. L. Ahlgren, M. J. Kalisher, J. B. James, and W. J. Hamilton, *Mater. Res. Soc. Symp. Proc.* **161**, 351 (1990).
- <sup>27</sup>D. W. Snyder, S. Mahajan, E. I. Ko, and P. J. Sides, *Appl. Phys. Lett.* **58**, 848 (1991).
- <sup>28</sup>S. K. Ghandhi, I. B. Bhat, H. Ehsani, D. Nucciarone, and G. Miller, *Appl. Phys. Lett.* **55**, 137 (1989).
- <sup>29</sup>I. Bhat, H. Ehsani, S. K. Ghandhi, D. Nucciarone, and G. Miller (unpublished).
- <sup>30</sup>P. R. Emtage, T. A. Temofonte, A. J. Noreika, and C. F. Seiler, *Appl. Phys. Lett.* **54**, 2015 (1989).